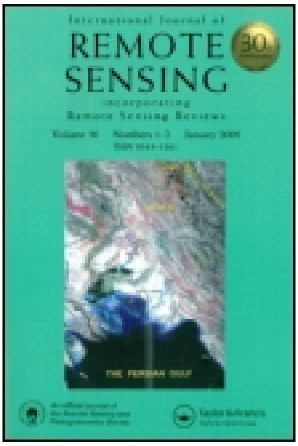

International Journal of Remote Sensing
Publication details, including instructions for authors and subscription information:
http://www.tandfonline.com/loi/tres20

Preliminary applications of a land surface temperature retrieval method to IASI and AIRS data

Xiaoying Ouyang [a b] , Guoting Kang [b] , Funian Zeng [c] , Enyun Qi [d] & Zhao-Liang Li [b e]

[a] State Key Laboratory of Remote Sensing Science, Jointly Sponsored by the Institute of Remote Sensing Applications of Chinese Academy of Sciences and Beijing Normal University, Beijing, 100101, China

[b] State Key Laboratory of Resources and Environmental Information System, Institute of Geographical Sciences and Natural Resources Research, Beijing, 100101, China

[c] China Aero Geophysical Survey & Remote Sensing Centre for Land and Resources, Beijing, 100083, China

[d] Harbin University of Science and Technology, Harbin, China

[e] LSIIT, UdS, CNRS, 67412, Illkirch, France

Published online: 30 Oct 2012.

International Journal of Remote Sensing, 2013
Vol. 34, Nos. 9–10, 3128–3139, http://dx.doi.org/10.1080/01431161.2012.716916

Preliminary applications of a land surface temperature retrieval method to IASI and AIRS data

Xiaoying Ouyang[a,b], Guoting Kang[b], Funian Zeng[c], Enyun Qi[d], and Zhao-Liang Li[b,e]*

[a]*State Key Laboratory of Remote Sensing Science, Jointly Sponsored by the Institute of Remote Sensing Applications of Chinese Academy of Sciences and Beijing Normal University, Beijing 100101, China;* [b]*State Key Laboratory of Resources and Environmental Information System, Institute of Geographical Sciences and Natural Resources Research, Beijing 100101, China;* [c]*China Aero Geophysical Survey & Remote Sensing Centre for Land and Resources, Beijing 100083, China;* [d]*Harbin University of Science and Technology, Harbin, China;* [e]*LSIIT, UdS, CNRS, 67412 Illkirch, France*

(*Received 28 December 2010; accepted 27 June 2011*)

Land surface temperature (LST) is one of the key state variables for many applications. This article aims to apply our previously developed LST retrieval method to infrared atmospheric sounding interferometer (IASI) and atmospheric infrared sounder (AIRS) data. On the basis of the opposite characteristics of the atmospheric spectral absorption and surface spectral emissivity, a 'downwelling radiance residual index' (DRRI) has been recalled and improved to obtain LST and emissivity. To construct an efficient DRRI, an automatic channel selection procedure has been proposed, and 11 groups of channels have been selected within the range 800–1000 cm^{-1}. The DRRI has been tested with IASI and AIRS data. For the IASI data, the radiosonde data have been used to correct for atmospheric effects and to retrieve LST, while the atmospheric profiles retrieved from AIRS data have been used to perform the atmospheric corrections and subsequently to estimate LST from AIRS data. The differences between IASI- and Moderate Resolution Imaging Spectroradiometer (MODIS)-derived LSTs are no more than 2 K, while the differences between AIRS- and MODIS-derived LSTs are less than 5 K. Even though an exceptionally problematic value occurred (–12.89 K), the overall differences between AIRS-estimated LST and the AIRS L2 LST product are no more than 5 K. Although the IASI-derived LST is more accurate than the AIRS-derived one, the convenient retrieval of AIRS atmospheric profile made this method more applicable. Limitations and uncertainties in retrieving LST using the DRRI method are also discussed.

1. Introduction

Land surface temperature (LST) and emissivity in the thermal infrared (TIR) spectral region are two important physical features of the land surface−atmosphere boundary system. Although remote sensing remains the best way to obtain them over a large area, retrieving LST and emissivity from multispectral TIR data cannot produce accurate temperature and emissivity simultaneously, due to complicated land surfaces and relatively inadequate measurement information. Spaceborne hyperspectral TIR sensors offer a great opportunity to resolve the temperature/emissivity separation (TES) problem.

*Corresponding author. Email: lizl@igsnrr.ac.cn

As indicated by Realmuto (1990), the core problem of TES is that we obtain N spectral measurements of radiance but need to find $N + 1$ unknowns (N emissivities and one temperature), even if the atmospheric perturbations have been well corrected for. This is a nondeterministic problem, and therefore at least one additional constraint must be found to obtain a realistic solution for the TES. Many methods of finding the appropriate constraint have been proposed, including the day–night measurement method which assumes equal surface emissivity at daytime and night, the greybody emissivity method which assumes constant channel emissivities, and the model emissivity method which resorts to an empirically linear relationship among channel emissivities (Kahle, Madura, and Soha 1980; Becker and Li 1990; Kealy and Gabell 1990; Realmuto 1990; Barducci and Pippi 1996; Wan and Li 1997; Gillespie et al. 1998). However, these methods are usually not universal and make it difficult to obtain accurate LST and emissivity for varying land-cover types using multispectral TES methods.

The launch of more hyperspectral sensors, such as the infrared atmospheric sounding interferometer (IASI) and atmospheric infrared sounder (AIRS), increases demands to retrieve LST and land surface emissivity (LSE) from remotely sensed data. The large number of narrower observation channels provided by hyperspectral sensors makes them a useful tool for exploiting information contained in discrete absorption features of both atmosphere constituents and land surface (Guanter, Richter, and Moreno 2006). Some contributions have delineated the virtues and features of using hyperspectral TIR measurements to separate LST and emissivity. A spectrally smooth emissivity (SSE) retrieval algorithm has been proposed by using the smoothness of the spectral emissivity defined by a sliding window and selecting the smoothest emissivity as the best estimation (Borel 1998). Smith et al. (1996) almost simultaneously proposed the spectral smoothness method to retrieve sea surface temperature (SST). Ingram and Muse (2001) analysed the systematic errors in the SSE algorithm of Borel (1998) and concluded that instrumental noise is the most important source of error. The frequent occurrences of singular value and low computational efficiency impede the application of the SSE method, which uses all the channels (more than 1000 for operational hyperspectral satellite data) in TIR for the calculations.

Atmospheric correction is of great importance in this study. Therefore, two types of atmospheric profiles – radiosonde observations and satellite retrievals – are chosen to correct for the atmospheric effect. However, both of them have advantages and limitations in applications. The satellite retrieved profiles are of high spatial-temporal coverage but poor vertical resolution and may suffer from uncertainties in calibration (Bates and Wu 1996). For the radiosonde observations, the profiles have high vertical resolution and a long historical record, but they are limited by their restricted spatial coverage, reduced accuracy in the upper troposphere (for certain locations, water vapour is not reported at all levels in the upper troposphere, while accurate radiative transfer calculations require water vapour profiles up to the 100 mb level), and inhomogeneities resulting from changes in instrumentation and reporting practices (Soden and Lanzante 1996). Although there are kinds of limitations, both satellite retrievals and radiosonde observations are still widely used to provide water vapour and temperature profiles for field campaigns and national observing networks (Soden et al. 2004).

In our previous study, we proposed a new index named 'downwelling radiance residual index' (DRRI) to give an additional constraint for the TES problem (Ouyang et al. 2010). This method allows for increased retrieval speed and avoids the problems of singular value. The validation in that work was only conducted with simulated data produced by other studies. In this article, data acquired from the operational hyperspectral satellite sensors IASI and AIRS are applied to further test the actual performance of the DRRI method. The IASI- and AIRS-derived LSTs are validated with Moderate Resolution

Imaging Spectroradiometer (MODIS) products on the basis of the atmospheric radiative transfer model (4A/OP, Operational Release for Automatized Atmospheric Absorption Atlas; http://ara.lmd.polytechnique.fr/).

This article is organized as follows. The DRRI method is recalled in Section 2.1. The channel selection procedure is presented in Section 2.2. The data used in this study are described in Section 3. Two application results of our DRRI method to retrieve LST from both IASI and AIRS data are presented in Section 4. Conclusions and perspectives are given in Section 5.

2. Method

2.1. Downwelling radiance residual index

Because the natural land surface is not a blackbody, at-ground leaving radiance contains both surface thermal emission and reflected atmospheric downwelling radiance. Surface emissivity spectra are always smooth, while atmospheric downwelling radiance spectra are jagged due to atmospheric absorption characteristics. If the LST is inaccurately estimated, the corresponding emissivity spectrum retrieved from at-ground radiance will exhibit a 'downwelling radiance residual feature'; in other words, sharp convexities or concavities caused by the atmospheric absorption lines in the estimated emissivity spectrum will appear. The DRRI was used to depict the direction and magnitude of the downwelling radiance residual feature and computed with the estimated emissivity values at several well-chosen channel groups. In these channel groups, peaks correspond to strong atmospheric line absorption, and valleys correspond to weak atmospheric absorption (Wang et al. 2008). The DRRI in a channel group (j) is given as:

$$\mathrm{DRRI}_j = \left((\varepsilon_1 - \varepsilon_2) + \frac{v_2 - v_1}{v_3 - v_1}(\varepsilon_3 - \varepsilon_1) \right)^2, \qquad (1)$$

where ε_2 is the estimated emissivity of the centre channel and ε_1 and ε_3 denote the estimated emissivity of the two shoulders in each group respectively and v is the wavenumber value of the three channels. Several three-channel group DRRIs constitute the final DRRI. According to the definition, the DRRI value is only a function of the estimated temperature. The Newton–Raphson algorithm (Press et al. 2007) was employed to find the corresponding LST, which is related to the solution of the equation, DRRI = 0. Once the LST was determined, the land surface spectral emissivities could be easily derived from the at-ground spectral leaving radiances. (Wang et al. 2008; Ouyang et al. 2010).

2.2. Automatic channel selection method

Figure 1 details the process of the automatic channel selection method in DRRI construction. To analyse the characteristics of the atmospheric downwelling radiance, 1413 cloud-free atmospheric profiles extracted from the Thermodynamic Initial-Guess Retrieval (TIGR; http://ara.abct.lmd.polytechnique.fr/index.php?page=tigr) database were used to simulate atmospheric downwelling spectral radiance with 4A/OP. Selection of the channels for constructing DRRI had to satisfy the following criteria.

(1) Atmospheric transmittance in the channel should be larger than 0.3; otherwise, atmospheric effects are so large that data measured by this channel could not contain enough information for the LST retrieval.

(2) The centre channel and the two bilateral channels should contrast in atmospheric absorption characteristics, with relatively strong absorption for the former and weaker absorption for the latter.
(3) Emissivities in these three channels (one centre plus two bilateral channels) have to be on one line. That is to say that three points (three channels) constructed by wavelength and emissivity should be collinear.

By taking into account these three constraints and examining the atmospheric downwelling spectral radiance and emissivity spectrum, 107 preliminary groups of three channels were selected. Subsequently, all 107 groups were further tested with simulated satellite data to find much better ones. Those groups could obtain estimated LST with the root mean square error (RMSE) at the minimum value for the simulated hyperspectral TIR data. Finally, 11 optimum groups of channels were selected to construct DRRI and retrieve LST. Table 1 shows the channel central positions of the 11 selected groups.

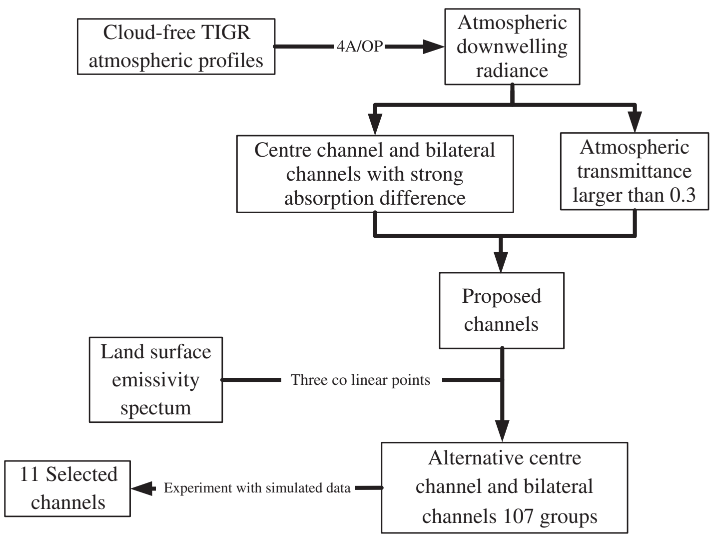

Figure 1. Automatic channel selection procedure.

Table 1. Position of channels for 11 selected groups.

Left (cm^{-1})	Centre (cm^{-1})	Right (cm^{-1})
802.25	803.25	804.25
823.75	825.25	826.25
826.00	827.75	830.25
831.75	840.00	841.25
847.00	849.50	851.75
851.00	852.50	854.00
920.00	922.25	923.75
923.75	925.00	926.50
947.00	948.25	949.00
975.00	976.00	976.75
976.50	977.25	978.00

The DRRI method requires at-ground radiance, atmospheric correction, and atmospheric downwelling spectral radiance to derive at-ground radiance from at-sensor radiance and retrieve LST. In this article, the atmospheric profiles for the atmospheric correction and the atmospheric downwelling radiance estimation are given either by radiosonde measurements or by the satellite products.

3. Data processes

3.1. Radiosonde measurement

In this study, the radiosounding data on 31 July 2008, obtained at Dal'Nerecensk (133.73° E, 45.87° N) are provided by the United Kingdom Meteorological Office (UKMO) at 0 and 12 h UTC. The UKMO data provide profiles of pressure, air temperature, and dew point temperature measured at 36 levels. 4A/OP requires the water vapour mixing ratio as input, so the dew point temperature was transformed to a mixing ratio.

3.2. IASI data

With 8461 spectral samples aligned in three regions between 645.0 and 2760 cm^{-1} (15.5 and 3.63 μm) and with a spectral resolution of 0.5 cm^{-1} and spectral sampling of 0.25 cm^{-1}, the IASI is a high-resolution Fourier transform spectrometer and is a key payload element of the METOP-A. The METOP-A is a European meteorological polar-orbit satellite funded by the European Organization for the Exploitation of Meteorological Satellites (EUMETSAT) and the European Space Agency member states and launched in 2006. IASI is expected to lead to dramatic improvements in the accuracy and height resolution of remotely sensed temperature and humidity profiles. The instantaneous field-of-view (IFOV) size at nadir is 12 km (http://www.eumetsat.int/Home/Main/Satellites/Metop/Instruments/SP_2010053151047495).

Procedures of the study area selection and IASI L1C data preparation are shown in Figure 2. The upper part is the procedure of the study area selection, while the bottom part is the IASI data preparation process.

In the study area selection, the MetOp two-line element was used to match the UKMO radiosonde data acquisition times (UTC time 0 and 12 h) with the IASI/MetOp-A acquisition time, so that the IASI data could be corrected for atmospheric effects with simultaneous atmospheric profiles. In this study, UKMO data and IASI measurements were all obtained at 0 h UTC. Excluding water (lake, ocean) and cloud-contaminated pixels, the satellite data at nadir with simultaneous atmospheric profiles were then used in our study.

The measurement data record (MDR) was derived from the selected IASI L1C data with the support of the IDL reader package. The sample width of IASI L1C spectra (IDefSpectDWn1b) and other sample information, as well as L1C spectra (GS1cSpect, top-of atmosphere (TOA) radiance) are stored in MDR. The other auxiliary data were also extracted with IASI TOA radiances (in MDR): Main Product Header Record (MPHR), Specific Product Header Record (SPHR), International Pointer Record (IPR), Global Internal Auxiliary Data Record (GIADR), Global External Auxiliary Data Record (GEADR), Variable Internal Auxiliary Data Record (VIADR), and Variable External Auxiliary Data Record (VEADR). MPHR and SPHR are the header products of the IASI product. MPHR includes the total count of all MDRs in the product (TOTAL_RECORDS). GIADR includes the scale factor, which is used in converting the original MDR to usable IASI TOA radiances.

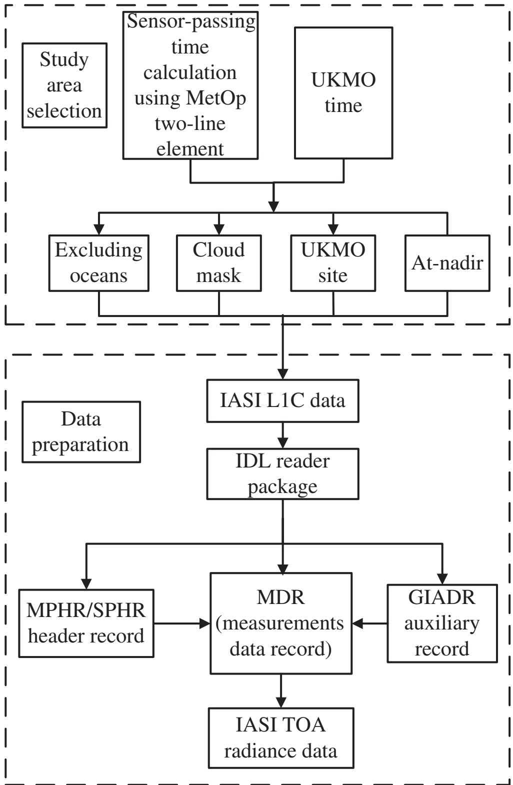

Figure 2. Scheme for study area selection and IASI data preparation I.

3.3. AIRS data

AIRS is a facility instrument aboard the second Earth Observing System (EOS) polar-orbiting platform, Aqua. Global coverage of AIRS data is obtained twice daily (day and night) on a 1:30 pm Sun-synchronous orbit at a 705 km altitude. The Aqua AIRS instrument is a cooled grating spectrometer with approximately 2500 spectral channels and a spectral resolving power of ~1200 (0.5–2 cm^{-1} spectral resolution) operating within the spectral range 650–2700 cm^{-1}.

The level-2 AIRS standard product consists of the cloud and surface properties, and the profiles of retrieved temperature, water vapour, ozone, carbon monoxide, and methane. Errors associated with these quantities are also part of the standard product. This product along with 4A/OP will give the real-time atmospheric parameters of AIRS TOA data. The vertical temperature profile has 28 levels in total with the corresponding pressure varying between 1100 and 0.1 mb, while the water vapour profile is reported to have 14 atmospheric layers with pressure between 1100 and 50 mb. The horizontal resolution is 0.5° (www-airs.jpl.nasa.gov).

3.4. MODIS LST product – MOD11B1/MYD11B1 data

The level-3 MODIS global LST and emissivity daily data are retrieved as 5 km grid data in a sinusoidal projected tile produced by the day/night LST algorithm from pairs of MODIS daytime and night observations in seven bands under certain conditions

(Wan and Li 1997). The MOD11B1/MYD11B1 product comprises the 6 km daytime and night LSTs, quality assessment, observation times, view angles, and emissivities retrieved in bands 20, 22–23, 29, and 31–32 (Wan 2008). Since the IFOVs of IASI and AIRS are 12 km and 0.5°, respectively, MOD11B1/MYD11B1 data should be re-sampled to the same pixel size for each data set in the bilinear convolution using MRT (https://lpdaac.usgs.gov/tools/modis_reprojection_tool/). In this study, one day of cloud-free MODIS data (31 July 2008) were chosen for the validation of IASI-derived LST and another set of cloud-free MODIS data from 11 August 2008 was chosen for the validation of corresponding AIRS-derived LST.

4. Results

LSTs were retrieved from IASI and AIRS data at nadir observation using our DRRI method. The atmospheric parameters (downwelling radiance, upwelling radiance, and transmittance) were estimated with 4A/OP for a spectral range varying from 800 to 1000 cm^{-1}. IASI and AIRS have different spectral resolutions and thus the spectral response function should be considered for different sensors.

4.1. LST retrieval from IASI data

Figure 3 shows the procedure of retrieving LST from IASI data and comparing IASI-derived LST with the MODIS LST product (MOD11B1). The input IASI data are the TOA radiance from 800 to 1000 cm^{-1} for each pixel, together with cloud information extracted from the IASI L2 product. The output data sets consist of the derived LST and LSE. The IASI L2 cloud product includes descriptions for cloud information, and in this article only the description of FLG_CLDSUM (clear, partly cloudy, or cloudy) is used. FLG_CLDSUM is the summary indicating which instruments see clouds (the IASI L2 product is obtained from several instruments including IASI, the Advanced TIROS Operational Vertical Sounders (ATOVS), and the Advanced Very High Resolution Radiometer (AVHRR)). In order to ensure the retrieval accuracy, the pixels masked as 'clear' are used in this article. Below is the description of each step involved in the procedure.

(1) *Extracting the values of IASI TOA radiance for each pixel*. Pixels masked by cloud and water surface were excluded in this study.
(2) *Calculating atmospheric parameters*. Because the correction of atmospheric effects is vital to the algorithm, the viewing geometry as well as atmospheric profiles (UKMO data at this part) were used as input to the 4A/OP atmospheric radiative transfer model.
(3) *Correcting atmospheric effects*. IASI TOA radiances together with the atmospheric parameters calculated above were then used to obtain the at-surface radiance and atmospheric downwelling radiance.
(4) *Estimating and validating LST*. As mentioned in Equation (1), the DRRI is calculated with the selected IASI channels to obtain LST and LSE. Since IASI IFOV at nadir is 12 km, it is difficult to perform the field validation over such a large area. The cross-validation was carried out by using the Terra−MOD11B1 5 km LST and LSE product. The MOD11B1 product is obtained at about local solar time 11:20, while IASI data are obtained at about local time 9:00 (UTC time 00:00 (the acquisition time of IASI data is same as that of radionsondes) + 09:00 (zone time of the

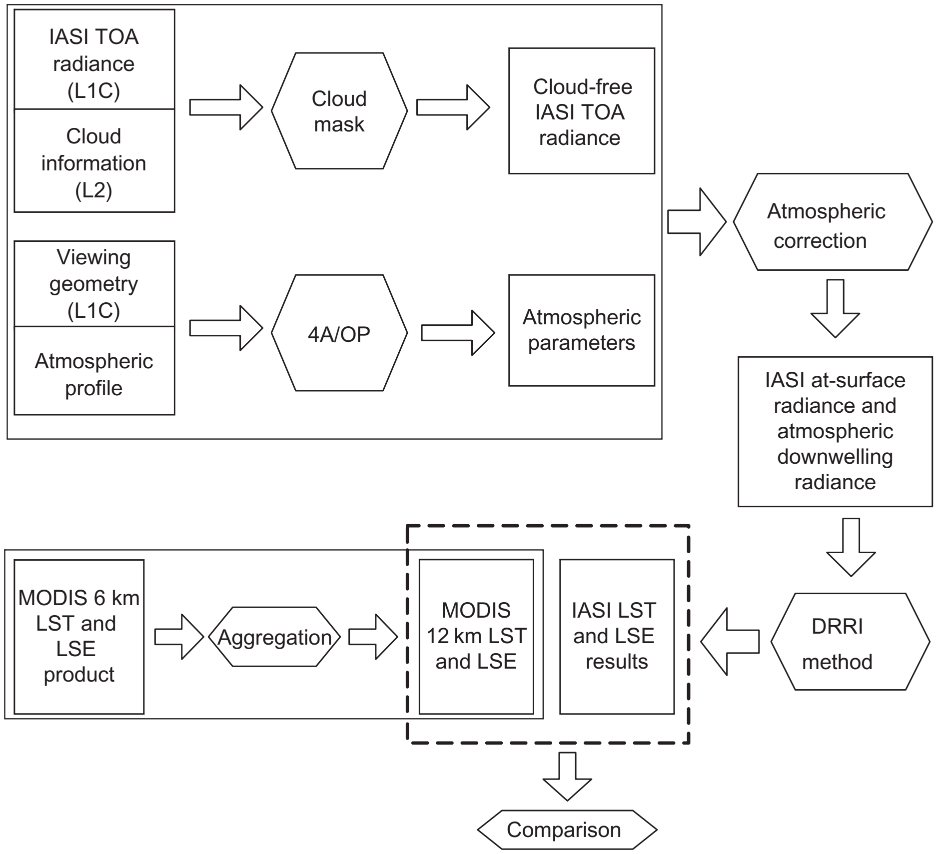

Figure 3. Procedures for retrieving LST from IASI data and comparing IASI-derived LST with the MODIS LST product (MOD11B1).

study area)). The time difference between the acquisition of the IASI and MODIS data is about 2 h.

Four pixels (all in an IASI measurement) near the Dal'Nerecensk radiosonde site in south-east Russia (Figure 4) were chosen as the validation sites for IASI data. The radiosounding data acquired near the locations of the four pixels (distances between them are no more than 30 km) were used to perform the atmospheric correction for all four pixels. Finally, the DRRI method was applied to derive LST from atmospherically corrected at-ground radiance.

Table 2 presents the comparison of LST estimated from 800 to 1000 cm^{-1} IASI TIR data using the above-mentioned DRRI procedure with the MOD11B1 LST product at the four sites of Dal'Nerecensk. Relatively good agreement was obtained. The estimated LSTs at nadir and Dal_2 were underestimated by 0.65 K and 2.05 K, respectively, in comparison with MOD11B1, while the estimated LSTs at Dal and Dal_1 were overestimated by 0.97 K and 1.45 K, respectively. The best result was obtained over homogeneous land surface as shown in Figure 4 for site nadir. This means that the DRRI method has the capability, to some degree, of estimating LST using the hyperspectral TIR satellite data under the condition that atmospheric correction is well performed.

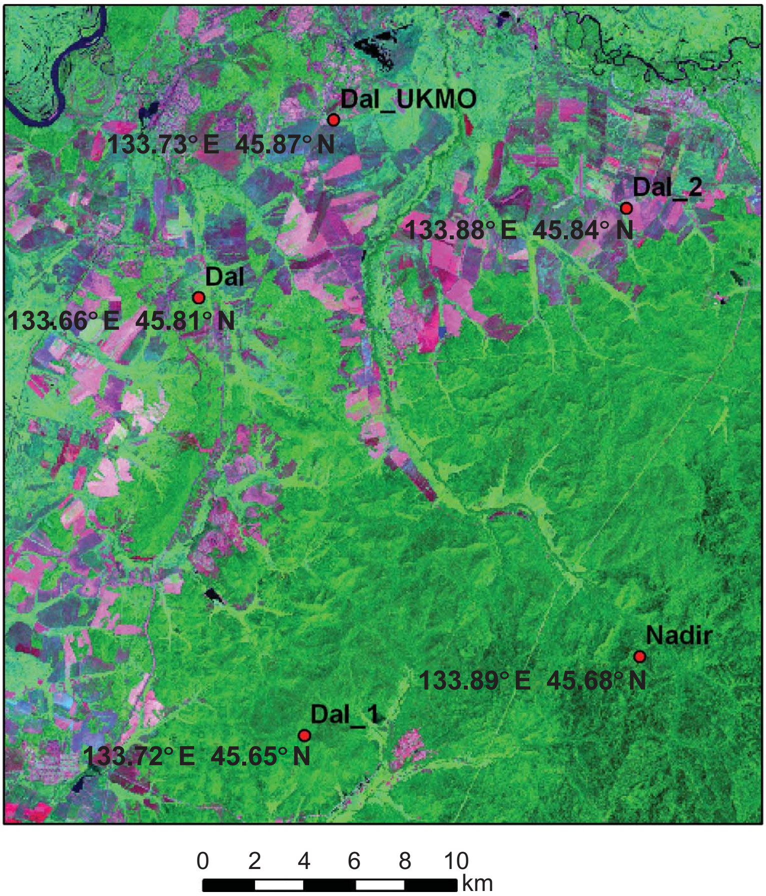

Figure 4. Locations of the four IASI pixels (Nadir, Dal, Dal_1, and Dal_2) and the UKMO radiosounding data site (Dal_UKMO) (31 July 2008). (Source: Landsat ETM +.)

Note: Land cover at Dal_2 is sparse vegetation; the cover at Nadir, Dal, and Dal_1 is all forest. (European Space Agency Ionia GlobCover Portal, http://ionia1.esrin.esa.int/.)

Table 2. Comparison of IASI-estimated LSTs with MOD11B1 values.

	Site			
	Nadir	Dal	Dal_1	Dal_2
Estimated LST (K)	291.45	291.47	291.49	287.99
MOD11B1(K)	292.10	290.50	290.04	290.04
Difference (K)	−0.65	0.97	1.45	−2.05

4.2. LST retrieval from AIRS data

Instead of the UKMO radiosonde data used in the IASI LST retrieval, the atmospheric temperature and water vapour profiles retrieved from AIRS were used in the AIRS LST retrieval process. Although the comparison of the IASI-estimated LST results with MOD11B1 data was good (as shown in Table 2), the different viewing zenith angle, azimuth

Table 3. Coordinates and land use for five selected samples for AIRS data.

	Site				
	A	B	C	D	E
Latitude	45.43° N	45.83° N	46.31° N	46.00° N	46.38° N
Longitude	110.66° W	111.34° W	111.52° W	109.46° W	111.00° W
Land use	Sparse vegetation	Cropland	Cropland	Grassland	Grassland

Table 4. Comparison of AIRS-estimated LSTs with MYD11B1 values.

	Site				
	A	B	C	D	E
Estimated LST (K)	304.76	303.95	304.68	314.68	304.68
AIRS L2 (K)	305.82	308.58	317.57	312.75	305.85
MYD11B1(K)	299.86	302.46	307.28	311.76	305.36
Estimated minus AIRS L2 (K)	−1.06	−4.63	−12.89	1.93	1.17
Estimated minus MYD11B1 (K)	4.90	1.49	−2.6	2.92	0.68

angle, and data acquisition caused by the IASI and MODIS payload satellites will impede the validation of IASI-derived LST results. Since AIRS and MODIS are two payloads on the same satellite (Aqua), the comparison of AIRS-estimated LST with MYD11B1 was more convincing. The level-2 cloud-free infrared AIRS radiances with IFOV of 0.5° were used here. A granule of 11 August 2008, (granule 204) was chosen to perform the LST retrieval. The view zenith angle effect at the centre place of the granule could be ignored. Five samples from North America were chosen and are shown in Table 3. Table 4 presents the results of LST estimated from 800 to 1000 cm^{-1} AIRS TIR data using the similar procedure to the above-mentioned DRRI procedure in Section 4.1 in comparison with the AIRS LST product (L2) and MODIS LST product (Aqua−MYD11B1). From this table, we realize that the DRRI-derived LST yielded less agreement with the AIRS product than the MODIS product. The estimated LST at site C was underestimated by 12.89 K in comparison with AIRS L2 product, while site B was underestimated by 4.63 K. The estimated LST of site A was overestimated by 4.9 K in comparison with MYD11B1 LST product. This was the poorest one in comparison to the MODIS product, at no more than 5 K. Similar to the IASI results, the worst result for AIRS came from sparse vegetation (other sites are all vegetation). That is to say our algorithm is still sensitive to the land use (LSE). This problem may be also due to the coarse resolution of AIRS atmospheric profiles, which impedes the atmospheric correction.

5. Conclusions

The new DRRI procedure for retrieving LST from hyperspectral satellite data is an improvement on the previous approaches. The main advantage is that the algorithm is fully automatic and optimal and suitable for processing the actual satellite data. The differences of IASI- and MODIS-derived LST are no more than 2 K, while the differences of AIRS- and MODIS-derived LST are less than 5 K. Although imperfect results have been obtained from the AIRS data, the convenient retrieval of AIRS atmospheric profiles makes the DRRI method more feasible for retrieving LST from the hyperspectral TIR data. However, it should be noted that all retrievals have been carried out for observations at nadir in this study. Uncertainties and errors would be greater for large viewing zenith angles.

Similar to the IASI results, the worst result for AIRS came from sparse vegetation (other sites are all vegetation). That is to say our algorithm is still sensitive to the land use (LSE). This problem may be also due to the uncertainty of atmospheric profiles, which impedes the atmospheric correction. However, these are only general guesses.

The atmospheric correction is very important for the DRRI method. As mentioned previously, both satellite measurements and radiosonde observations have limitations. The uncertainty of atmospheric profiles could not ensure the accuracy of atmospheric correction; therefore, biases of the estimated LST and emissivity remain great. The singular values are also caused by the inaccurate atmospheric correction and estimated LST. However, only a few sites have been analysed in this preliminary work, and more case studies have to be performed in the near future. More validation will be made in other sites, especially with various atmospheric profiles such as numerical weather prediction (NWP) data. The NWP global data are useful in areas where no observation is available. More validation will also be done with IASI temperature and humidity profiles extracted from IASI data to eliminate problems concerning the combination with radiosondes.

Acknowledgements

The authors thank the anonymous referees for their comments and suggestions that have significantly improved the article. This work was partly supported by the Hi-Tech Research and Development Programme of China (863 Plan Programme) under Grants 2008AA121805 and 2006AA12Z121, and by the State Key Laboratory of Resource and Environment Information System under Grant 088RA800KA. The authors sincerely thank NOVELTIS Inc. for providing the 4A/OP model and the Laboratoire de Meteorologie Dynamique for providing the TIGR database.

References

Barducci, A., and I. Pippi. 1996. "Temperature and Emissivity Retrieval from Remotely Sensed Images Using the 'Grey Body Emissivity' Method." *IEEE Transactions on Geoscience and Remote Sensing* 34: 681–95.

Bates, J. J., and X. Wu. 1996. "Interannual Variability of Upper-Troposphere Water Vapour Band Brightness Temperature." *Journal of Climate* 9: 427–38.

Becker, F., and Z.-L. Li. 1990. "Temperature-Independent Spectral Indices in Thermal Infrared Bands." *Remote Sensing of Environment* 32: 17–33.

Borel, C. C. 1998. "Surface Emissivity and Temperature Retrieval for a Hyperspectral Sensor." In *Proceedings of the IEEE International Geoscience and Remote Sensing Symposium*, IGARSS 1998, Seattle, WA, July 6–10, 1998, Vol. 1, 546–9.

Gillespie, A. R., T. Matsunaga, S. Rokugawa, and S. J. Hook. 1998. "A Temperature and Emissivity Separation Algorithm for Advanced Spaceborne Thermal Emission and Reflection Radiometer (ASTER) Images." *IEEE Transactions on Geoscience and Remote Sensing* 36: 1113–26.

Guanter, L., R. Richter, and J. Moreno. 2006. "Spectral Calibration of Hyperspectral Imagery Using Atmospheric Absorption Features." *Applied Optics* 45: 2360–70.

Ingram, P. M., and A. H. Muse. 2001. "Sensitivity of Iterative Spectrally Smooth Temperature/Emissivity Separation to Algorithmic Assumptions and Measurement Noise." *IEEE Transactions on Geoscience and Remote Sensing* 39: 2158–67.

Kahle, A. B., D. P. Madura, and J. M. Soha. 1980. "Middle Infrared Multispectral Aircraft Scanner Data: Analysis for Geological Applications." *Applied Optics* 19: 2279–90.

Kealy, P. S., and A. R. Gabell. 1990. "Estimation of Emissivity and Temperature Using Alpha Coefficients." In *Proceedings of 2nd TIMS Workshop*, edited by Elsa A. Abbott, June 6, 1990. Pasadena, CA: JPL Publication 90–55.

Ouyang, X. Y., N. Wang, H. Wu, and Z.-L. Li. 2010. "Errors Analysis on Temperature and Emissivity Determination from Hyperspectral Thermal Infrared Data." *Optics Express* 18: 544–50.

Press, W. H., B. P. Flannery, S. A. Teukolsky, and W. T. Vetterling. 2007. *Numerical Recipes: The Art of Scientific Computing*. New York, NY: Cambridge University Press.

Realmuto, V. J. 1990. "Separating the Effects of Temperature and Emissivity: Emissivity Spectrum Normalization." In *Proceedings of 2nd TIMS Workshop*, edited by Elsa A. Abbott, June 6, 1990. Pasadena, CA: JPL Publication 90–55.

Smith, W. L., R. O. Knuteson, H. E. Revercomb, and W. Feltz. 1996. "Observations of the Infrared Radiative Properties of the Ocean-Implications for the Measurement of Sea Surface Temperature via Satellite Remote Sensing." *Bulletin of the American Meterological Society* 77: 41–51.

Soden, B. J., and J. R. Lanzante. 1996. "An Assessment of Satellite and Radiosonde Climatologies of Upper-Tropospheric Water Vapour." *Journal of Climate* 9: 1235–50.

Soden, B. J., D. D. Turner, B. M. Lesht, and L. M. Miloshevich. 2004. "An Analysis of Satellite, Radiosonde, and Lidar Observations of Upper Tropospheric Water Vapour from the Atmospheric Radiation Measurement Program." *Journal of Geophysical Research* 109: D04105. doi:10.1029/2003JD003828.

Wan, Z. M. 2008. "New Refinements and Validation of the MODIS Land-Surface Temperature/Emissivity Products." *Remote Sensing of Environment* 112: 59–74.

Wan, Z. M., and Z.-L. Li. 1997. "A Physics-Based Algorithm for Retrieving Land-Surface Emissivity and Temperature from EOS/MODIS Data." *IEEE Transactions on Geoscience and Remote Sensing* 35: 980–96.

Wang, X., X. Y. Ouyang, B. H. Tang, Z.-L. Li, and R. H. Zhang. 2008. "A New Method for Temperature/Emissivity Separation from Hyperspectral Thermal Infrared Data." In *Proceedings of IEEE International Geoscience and Remote Sensing Symposium*, IGARSS 2008, Boston, MA, July 8–11, 2008, III, 286–9.